3504–3517 Nucleic Acids Research, 2013, Vol. 41, No. 6 Published online 4 February 2013
doi:10.1093/nar/gkt049

Acetylated Histone H3K9 is associated with meiotic recombination hotspots, and plays a role in recombination redundantly with other factors including the H3K4 methylase Set1 in fission yeast

Shintaro Yamada[1,2], Kunihiro Ohta[1,2] and Takatomi Yamada[1,*]

[1]Department of Life Sciences, Graduate School of Arts and Sciences, The University of Tokyo, Tokyo 153-8902, Japan and [2]Department of Biophysics and Biochemistry, Graduate School of Science, The University of Tokyo, Tokyo 113-0032, Japan

Received September 14, 2012; Revised December 25, 2012; Accepted January 12, 2013

ABSTRACT

Histone modifications are associated with meiotic recombination hotspots, discrete sites with augmented recombination frequency. For example, trimethylation of histone H3 lysine4 (H3K4me3) marks most hotspots in budding yeast and mouse. Modified histones are known to regulate meiotic recombination partly by promoting DNA double-strand break (DSB) formation at hotspots, but the role and precise landscape of involved modifications remain unclear. Here, we studied hotspot-associated modifications in fission yeast and found general features: acetylation of H3 lysine9 (H3K9ac) is elevated, and H3K4me3 is not significantly enriched. Mutating H3K9 to non-acetylatable alanine mildly reduced levels of the DSB-inducing protein Rec12 (the fission yeast homologue of Spo11) and DSB at hotspots, indicating that H3K9ac may be involved in DSB formation by enhancing the interaction between Rec12 and hotspots. In addition, we found that the lack of the H3K4 methyltransferase Set1 generally increased Rec12 binding to chromatin but partially reduced DSB formation at some loci, suggesting that Set1 is also involved in DSB formation. These results suggest that meiotic DSB formation is redundantly regulated by multiple chromatin-related factors including H3K9ac and Set1 in fission yeast.

INTRODUCTION

Histones package eukaryotic DNA into a highly condensed chromatin structure and impact all aspects of DNA-templated processes. Once incorporated into nucleosomes, histones sterically keep DNA-processing enzymes away from DNA and thereby inhibit DNA-related events. Consistently, *cis*-elements such as transcriptional promoters are often devoid of nucleosomes, and histones are transiently evicted from sites of transcription or repair (1). Histones also regulate the behaviour of chromatin-structured DNA through post-translational modifications by affecting histone–DNA interactions or by recruiting other proteins. Various modifications such as acetylation and methylation are known to date, and each modification is related to one or several DNA-templated reactions. For example, acetylation of histones and methylation of histone H3 lysine4 (H3K4), often observed in active chromatin regions, are involved in the activation of transcription (2).

Homologous recombination, a process in which genetic information is exchanged between homologous DNA duplexes, is markedly activated during meiotic prophase. Meiotic recombination contributes to ensuring proper chromosome segregation as well as conferring genetic diversity to gametes and is essential to most sexually reproducing organisms. Not surprisingly, its failure can lead to consequences like infertility or birth defects. Furthermore, as this type of recombination is triggered by programmed DNA double-strand breaks (DSBs) that can be detrimental to cells, it must be initiated in a strictly regulated manner. Therefore, it is important to fully understand how meiotic recombination occurs *in vivo*: how are meiotic DSBs formed in the chromatin structure? Notably, meiotic DSBs are introduced by the conserved type II topoisomerase-like protein Spo11 (3), whose access to DNA is influenced by chromatin structure (4), and hence, meiotic DSBs occur predominantly in discrete sites called recombination hotspots. Because of their importance in recombination regulation, hotspots have been intensively studied.

Several traits of histones are known to be associated with meiotic recombination hotspots. First, hotspots

*To whom correspondence should be addressed. Tel: +81 3 5454 6655; Fax: +81 3 5465 8834; Email: takayamada@bio.c.u-tokyo.ac.jp

often reside in chromatin sites with less histone density such as nucleosome-depleted regions (4). Most hotspots in budding yeast coincide with transcriptional promoter regions (5) that contain fewer nucleosomes, and fission yeast hotspots are also devoid of histones (6). These observations would suggest that histones should be depleted around hotspots to allow the action of recombination factors including Spo11. This idea is supported by chromatin remodelling at the fission yeast hotspot *ade6-M26*. *M26* is a G:T nonsense point mutation (7,8), which creates a cyclic AMP (cAMP) response element-related '*M26*-sequence' (5′-ATGACGT-3′) that is bound by the activating transcription factor (ATF)/cAMP response element binding (CREB) family transcription factor dimer Atf1-Pcr1 (Figure 1A) (9,10). Recombination at this locus is dependent both on the *M26* sequence as well as Atf1-Pcr1 binding and is also proposed to be facilitated by chromatin alteration, which exposes embedded DNA around *ade6-M26* (11).

Another characteristic of histones near hotspots is an enrichment of post-translational modifications. For example, budding yeast hotspots are associated with histone H3 lysine9 acetylation (H3K9ac) and H3K4 trimethylation (H3K4me3) (12,13). In particular, H3K4me3 has been more extensively analysed, and deleting the sole H3K4 methyltransferase gene *SET1* results in a massive reduction in DSB formation (14). Similarly, a vast majority of hotspots carry H3K4me3 in mice (15,16) and, the meiotic H3K4 trimethylase PRDM9 is important for defining recombination hotspot distribution in mouse and human (17–19). Around the fission yeast *ade6-M26* hotspot, histones are more acetylated than around its negative control locus *ade6-M375*, and such hyperacetylation promotes DSB formation (20).

Although studies on various model organisms report the involvement of histones and their modifications in meiotic recombination, several crucial points remain elusive. For instance, the exact functions of hotspot-associated histone modifications are not yet known. Although H3K4me3 is proposed to be a possible determinant of hotspots in budding yeast and mouse, it does not overlap with all hotspots and *vice versa*. In addition, at least some DSBs can still be detected in *set1*-deleted budding yeast and Prdm9$^{-/-}$ mice, where H3K4me3 associated with authentic hotspots is largely eliminated (12,21,22). Moreover, further scrutiny of H3K4me3 around budding yeast hotspots increased the possibility that the modification may be due to colocalization of promoters and hotspots in this organism (23). These observations lead to the assumption that additional factors such as other histone modifications may exist around hotspots (16). It is also unclear how conserved these hotspot-associated modifications are across species.

Seeking clues to understand the relation between hotspots and modified histones, we used fission yeast to examine hotspot-associated histone modifications and their possible roles. From analyses focused on several *M26*-sequence-dependent hotspots as well as the whole genome, we found that hotspots are generally enriched with H3K9ac. Eliminating H3K9ac partially decreases Rec12 levels and DSB formation at most hotspots. We also found that hotspots in fission yeast are not associated with H3K4me3, but that deletion of the H3K4 methyltransferase gene *set1* causes increased Rec12 binding to chromatin and reduced DSB formation at some loci. These results point to a possibility that H3K9ac and Set1 are both, but differently, involved in meiotic DSB formation. They also suggest that other factors are likely to play a part in meiotic recombination, given the partial defects in the mutants of H3K9ac and Set1. We speculate that multiple factors including H3K9ac and Set1 play various roles in meiotic DSB formation in fission yeast. Our present results will provide novel insights into the mechanism of meiotic recombination.

MATERIALS AND METHODS

Yeast strains and general methods

Strains used in this study are listed in Supplementary Table S1. Procedures for strain constructions are described in Supplementary Materials and Methods. Spore viability was measured by micromanipulating spontaneously released spores with the SINGER MSM system (Singer), and meiotic recombination frequency was measured by random-spore analyses. The binomial test was used for Figure 4D, and the *t*-test was used for all other statistical analyses. Throughout the article, statistical significance is indicated as $*P < 0.05$, $**P < 0.01$ and $***P < 0.001$.

Detection of meiotic DSBs and Rec12-oligonucleotides

Meiotic DSBs except for those at *hsp10* were detected as previously described (24,25). DSBs at *hsp10* were detected by digesting genomic DNA with *Nru* I followed by southern hybridization. The hybridization probe was polymerase chain reaction (PCR) amplified from *Schizosaccharomyces pombe* genomic DNA using the primers 5′-GTCAGCATGCTCTAGTAGGGTTATTGG-3′ and 5′-TCGTTTAAGAAGCTGTGATTGTTCACG-3′. Rec12-oligonucleotides complexes were detected as in (26).

Chromatin immunoprecipitation quantitative real-time PCR

Chromatin immunoprecipitation (ChIPs) were performed as previously described (20). Antibodies used are described in Supplementary Materials and Methods, and the specificities of anti-H3K9ac and -H3K4me3 antibodies were confirmed by western blotting (data not shown). To calculate histone modification levels, DNA immunoprecipitated with anti-modified histones and histone H3 was analysed by quantitative real-time PCR (qPCR) using the Applied Biosystems 7500 Real-Time PCR system. The results were analysed as follows. First, signal intensities obtained with modified histones were divided by those with histone H3. For example, H3K9ac at *ade6-M26* was calculated according to the formula below.

$$\mathrm{K9ac@}M26/\mathrm{H3cter@}M26$$

Also calculated were relative histone modification levels at the analysed loci normalized to those at the internal

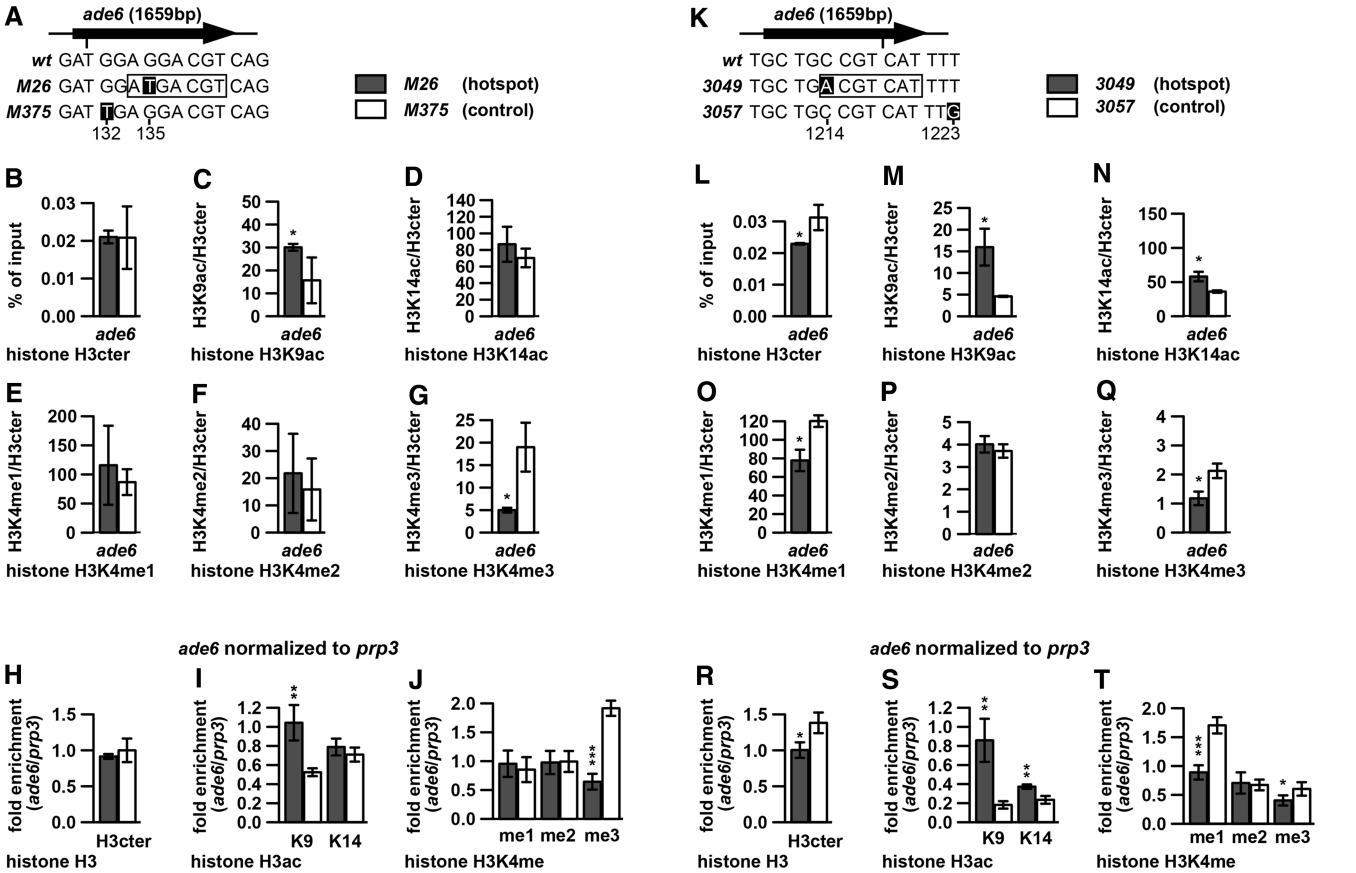

Figure 1. Histone H3 and modified histones at *M26*-sequence-dependent hotspots, *ade6-M26* and *ade6-3049*. The ade*6-M26*, *ade6-M375*, *ade6-3049* and *ade6-3057* cells in the haploid *pat1-114* background were induced into meiosis and harvested 1 h after the induction. ChIP experiments were performed using an antibody specific to the histone H3 core domain, and antibodies specific to the modifications are shown underneath the *x*-axis. DNA isolated from immunoprecipitates and whole-cell extracts was analysed by real-time qPCR, where fragments corresponding to the hotspot or control loci (*ade6*), and the *prp3*$^+$ promoter (*prp3*) were amplified. (**A–J**) Histone H3 and modified histone levels at *ade6-M26* (filled bars) and *ade6-M375* (open bars). (A) Positions of *ade6-M26* and *ade6-M375* within the *ade6* gene and sequences around the two loci. The rectangle and white lettering indicate the *M26*-sequence and mutated bases, respectively. The numbers below the sequences indicate nucleotide position, with the first 'A' of the *ade6* ORF as 1. (B) Histone H3 levels were calculated as the percentage of DNA fragments in histone H3cter immunoprecipitates relative to those in whole-cell extract and shown in the *y*-axis. (C–G) Histone modification levels were calculated by dividing signal intensities of modified histone immunoprecipitates with those of histone H3 immunoprecipitates and shown in the *y*-axes. The means and standard deviations from three independent experiments are shown. (C) H3K9ac levels. (D) H3K14ac levels. (E) H3K4me1 levels. (F) H3K4me2 levels. (G) H3K4me3 levels. (H) Relative Histone H3 levels at the *ade6* locus normalized to *prp3*. 'Fold enrichment' values were calculated for individual experiments. Their means and standard deviations are shown. (I and J) Relative histone modification levels at *ade6* normalized to *prp3*. 'Fold enrichment' values were calculated for individual experiments. Their means and standard deviations are shown. (I) H3K9ac (K9) and H3K14ac (K14) levels. (J) H3K4me1 (me1), H3K4me2 (me2) and H3K4me3 (me3) levels. (**K–T**) Histone H3 and modified histone levels at *ade6-3049* (filled bars) and *ade6-3057* (open bars). (K) Positions of *ade6-3049* and *ade6-3057* within the *ade6* ORF and sequences around the two loci. The rectangle, white lettering and numbers below the sequences are as in (A). Note that the *M26*-sequence at *ade6-3049* is on the complementary strand. (L) Histone H3 levels were calculated and shown as in (B). (M–Q) Histone modification levels were calculated and shown as in (C–G). (M) H3K9ac levels. (N) H3K14ac levels. (O) H3K4me1 levels. (P) H3K4me2 levels. (Q) H3K4me3 levels. (R) Histone H3 levels at the *ade6* locus were calculated and shown as in (H). (S and T) Relative histone modification levels at *ade6* were calculated and shown as in (I and J). (S) H3K9ac (K9) and H3K14ac (K14) levels. (T) H3K4me1 (me1), H3K4me2 (me2) and H3K4me3 (me3) levels.

control locus, *prp3*$^+$ promoter region. For example, fold enrichment of H3K9ac at *ade6-M26* was calculated according to the formula below.

(K9ac@*M*26/H3cter@*M*26) / (K9ac@*prp*3/H3cter@*prp*3)

To calculate Rec12 levels, the formula below was used.

Rec12@*M*26 / Rec12@*prp*3

Used primers are listed in Supplementary Table S2. All experiments were performed three times from independent cell cultures.

ChIP-chip

ChIPs were performed as previously described (20). DNA from whole-cell extracts, and ChIP fractions were amplified and end-labelled with the in vitro transcription (IVT) Amplification Method described elsewhere (27). Each sample was analysed using a GeneChip® *S. pombe* Tilling 1.0 FR Array (P/N 900647, Affymetrix) as described in the Affymetrix® Chromatin Immunoprecipitation Assay Protocol (P/N 702238 Rev. 3). Signals were quantile normalized and smoothed with a half window size of 250 bp (histones) and 375 bp (Rec12) using Two Sample

Comparison Analysis of an Affymetrix® Tiling Analysis Software. For Supplementary Figure S10A–C, in which we compared Rec12 signal strengths from independent experiments, data were normalized to standard deviation and median and smoothed with a half window size of 375 bp.

(Histones) ChIP signals obtained with the anti-histone H3cter antibody were normalized to those with DNA in whole-cell extract. These scores were then used to normalize ChIP signals obtained with the anti-histone H3K9ac, H3K14ac and H3K4me3 antibodies. Sites with enriched modified histones were determined by using MA of CisGenome (28) [One Sample Comparison, (W) = 0, (Window Boundary) = 250, (Region Boundary Cutoff, MA>) = 0.3, (Maximum Gap within a Region) = 250, (Maximum Run of Insignificant Probes within a Region) = 5, (Minimum Region Length) = 250, (Minimum Number of Significant Probes within a Region) = 15].

(Rec12) ChIP signals obtained with the anti-FLAG antibody were normalized to those in whole-cell extract. Rec12 binding sites were determined by using MA of CisGenome (28) [One Sample Comparison, (W) = 0, (Window Boundary) = 375, (Region Boundary Cut-off, MA >) = 0.6, (Maximum Gap within a Region) = 375, (Maximum Run of Insignificant Probes within a Region) = 7.5, (Minimum Region Length) = 375, (Minimum Number of Significant Probes within a Region) = 22.5].

The region around the *ade6* gene (chr3: 1312712-1325203) and the *set1* gene (chr3: 412000-417000), 100 kb regions from each end of every chromosome, centromeres (chr1: 3752000-3792000; chr2: 1595000-1650000; chr3: 1060000-1150000) and mating-type loci (chr2: 2110000-2140000) and SPBPJ4664.02 gene (chr2: 688616-700531), which were excluded from analyses in a previous study (29) owing to the difference in genotype and the low density of probes used in ChIP-chip data, were not analysed in this study either. Two closely positioned binding sites were merged, provided that the corresponding region in another strain contains a single binding site.

S. pombe sequence information was according to the Wellcome Trust Sanger Institute (September 2004). The raw and processed data for the ChIP-chip analyses are deposited at the Gene Expression Omnibus (GEO accession number GSE31648).

RESULTS

Detailed histone modifications around the *ade6-M26* recombination hotspot

To gain clues for globally analysing hotspot-associated modifications, we first focused on several *M26*-sequence-dependent hotspots to test which lysine residues are specifically acetylated and whether H3K4 is methylated. Modification levels at hotspots and their respective non-hotspot control loci were compared by ChIP. For accurate detection of subtle difference associated with meiotic recombination, we designed the experimental system as follows. (i) The highly synchronous *pat1-114* haploid meiosis system was adopted (For details, see Supplementary Materials and Methods). As we previously observed that the difference in acetylation levels between *M26* and *M375* is more prominent in early meiosis (20), cells harvested 1 h after meiosis induction were analysed. (ii) A limited region (~100 bp) encompassing *M26* or *M375* was analysed by qPCR. (iii) To correct for differences in nucleosome occupancy among analysed loci, ChIP experiments were also performed using an antibody against the C-terminal domain of histone H3 (H3cter). The modified histone signals were normalized to H3cter signals.

We observed that both *ade6-M26* and *ade6-M375* are located in a region with less nucleosomes (Supplementary Figure S1; see later in the text and Supplementary Figure S12 for details) and did not show a significant difference in histone H3 levels (Figure 1B). Remarkably, H3K9 was more acetylated around *M26* than around *M375* (Figure 1C, *t*-test, $P = 0.048$), whereas H3K14 was acetylated at comparable levels between the two loci (Figure 1D). Four lysines of histone H4 were also tested for acetylation: lysine5 (H4K5), 8 (H4K8), 12 (H4K12) and 16 (H4K16). Although the lysines other than H4K5 seemed to be more acetylated at *M26* than at *M375*, the differences were not significant (Supplementary Figure S2A–D). Extending our analysis to other modifications, we examined the distinct H3K4 methylation states; mono (H3K4me1), di (H3K4me2) and H3K4me3 (Figure 1E–G). ChIP analyses revealed that H3K4me1 and H3K4me2 levels were similar between *M26* and *M375*. However, H3K4me3 was less enriched around *M26*, the hotspot locus, than around *M375*, the control locus ($P = 0.034$).

ChIP consists of many steps that can intrinsically cause variability between samples. Such sample-to-sample difference can be considered by simultaneous analyses of an internal control locus to discuss histone modification patterns between hotspots and their control sites. For this purpose, a fragment of the promoter region of $prp3^+$, which is on a different chromosome from the *ade6* gene (*prp3* is on the Chromosome I and *ade6* is on the Chromosome III), was mainly used. This region was in a similar chromatin status between hotspot-containing strains and their control strains (Supplementary Figure S3). Relative modification levels at the hotspot (or control) loci were calculated for individual experiments by normalizing the modified histone/H3cter ratio of *ade6* fragments to that of $prp3^+$. Then, the averages and standard deviations were calculated (Figure 1H–J). By this analysis, we confirmed that histone H3K9ac is more enriched at *M26* than at *M375* ($P = 0.0046$) and that H3K4me3 is lower at *M26* than at *M375* ($P = 0.00016$). Such a tendency of H3K4me3 was constantly observed throughout early meiosis, as the modification levels remained constant both at *M26* and *M375* during the time course (Supplementary Figure S4). We also tested, aside from $prp3^+$ aforementioned, the ORFs of $act1^+$ and $lys1^+$ as an internal control, and these two loci gave indistinguishable results from Figure 1H–J (Supplementary Figure S5). Taken together, we

hypothesized that a high level of H3K9ac and a low level of H3K4me3 might define chromatin around the *ade6-M26* hotspot.

Histone modifications around an *M26*-sequence-dependent hotspot close to the 3′-end of the *ade6* gene

Because *M26* is close to the promoter of the *ade6* gene (Figure 1A), and histone modification patterns are influenced by their relative locations along ORFs (2), we analysed another *M26*-sequence-dependent hotspot *ade6-3049*, which is located near the 3′-end of the *ade6* gene (Figure 1K). This time, *ade6-3057* was used as a non-hotspot control. Histone H3 was less associated with the *3049* hotspot than the *3057* control locus (Figure 1L and R). The modification levels normalized to histone occupancy demonstrated that acetylation patterns at *ade6-3049* are similar to those at *ade6-M26*: among the six acetylated lysines tested, H3K9ac was the most enriched at the hotspot (Figure 1M, N and S and Supplementary Figure S2E–H). We also checked H3K4 methylation and found that H3K4me1 and H3K4me3 were higher at *ade6-3057* than at *ade6-3049*, and that the H3K4me2 level between both loci was similar (Figure 1O, P, Q and T). This observation indicates that the *3049* hotspot did not show any degree of higher H3K4me compared with the negative control locus. The results on *M26* and *3049* highlight two findings about histone modifications that could characterize *M26*-sequence-dependent hotspots. First, H3K9ac is more tightly associated with these two hotspots than all other lysine acetylations tested. Second, in contrast to observations in budding yeast and mammals, H3K4me3 levels are not elevated around these recombination hotspots.

Histone modifications around a natural *M26*-sequence-dependent hotspot and in meiotic diploid cells

We wanted to know whether the aforementioned findings apply to more physiological conditions. First, we focused on the natural *M26*-sequence-dependent hotspot *cds1-M26*$_{ES}$*-I3*, which is located in an intron of the *cds1*$^+$ gene and is activated by Atf1-Pcr1 (25). A point mutation (*cds1-2*) within the *M26* sequence abolishes recombination activity (Figure 2A) (25). Using the *pat1-114* meiosis system, we compared the levels of histone H3 (Figure 2B), H3K9ac, H3K14ac and three degrees of H3K4me around the *cds1-M26*$_{ES}$*-I3* hotspot and *cds1-2*. As shown in Figure 2C, H3K9 was more acetylated at the hotspot than at the control locus ($P = 0.017$), whereas the levels of H3K14ac were similar. Moreover, H3K4me levels at all degrees were lower around the hotspot than around the *cds1-2* control locus (Figure 2D) ($P = 0.0051$ for me1; $P = 0.017$ for me2; $P = 0.0060$ for me3). Therefore, a natural *M26*-sequence-dependent hotspot showed similar H3K9ac and H3K4me patterns to those around *ade6* hotspots.

In *pat1-114* cells, meiosis is synchronously induced by activation of Mei2, a master regulator of meiosis entry, through heat inactivation of the meiosis-inhibiting Pat1 kinase (30). Although this system is widely used to analyse meiotic recombination in *S. pombe*, it might be

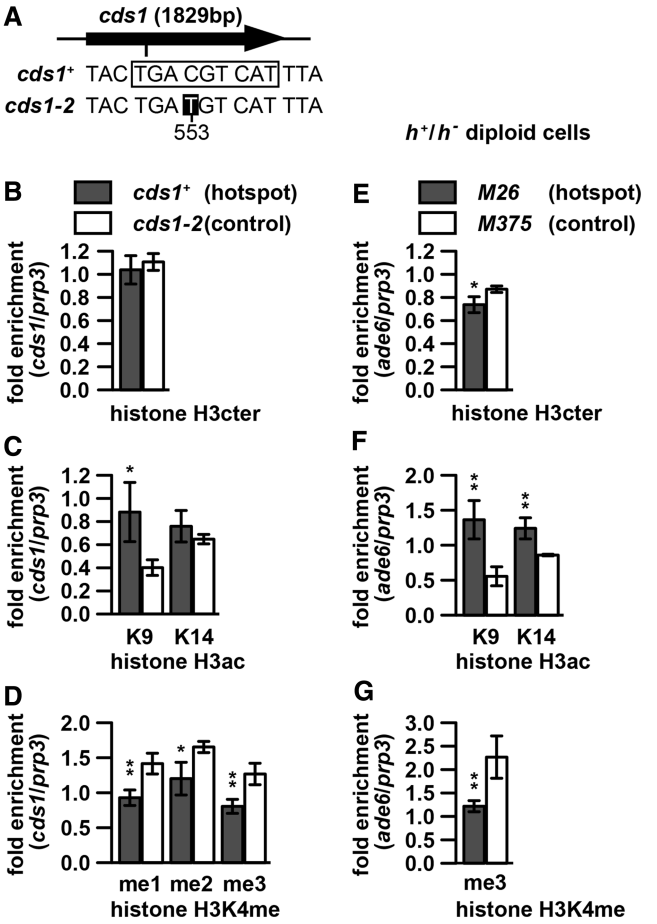

Figure 2. Histone H3 and its modifications at the natural *M26*-sequence-dependent hotspot *cds1-M26*$_{ES}$*-I3* and at *ade6-M26* in meiotic diploid cells. (**A–D**) Histone H3 and its modification levels around *cds1-M26*$_{ES}$*-I3* (*cds1*$^+$, filled bars) and *cds1-2* (open bars). *cds1*$^+$ and *cds1-2* cells in a *pat1-114* background were cultured, and histone H3 and its modification levels were assessed by ChIP as in Figure 1H–J. (A) Positions of *cds1-M26*$_{ES}$*-I3* and *cds1-2* within the *cds1* gene and sequences around the two loci. The rectangle and white lettering indicate the *M26*-sequence and mutated base, respectively. '553' indicates nucleotide position, with the first 'A' of the *cds1* ORF as 1. Note that the *M26*-sequence at *cds1-M26*$_{ES}$*-I3* is present on both strands. (B) Levels of Histone H3 (C) Levels of H3K9ac and H3K14ac. (D) Levels of H3K4me1, H3K4me2 and H3K4me3. (**E–G**) Histone H3 and its modification levels in h^+/h^- meiotic cells around *ade6-M26* (filled bars) and *ade6-M375* (open bars). The *ade6-M26* and *ade6-M375* h^+/h^- diploid cells were induced to enter meiosis by nitrogen withdrawal and harvested 3 h after the induction. Histone H3 and its modification levels were assessed by ChIP as in Figure 1H–J. (E) Levels of Histone H3. (F) Levels of H3K9ac and H3K14ac. (G) Levels of H3K4me3.

possible that histone modification patterns are affected by the artificial meiosis. To exclude this possibility, we performed similar experiments in h^+/h^- diploid cells induced into meiosis by nitrogen withdrawal. In these cells, nutritional starvation activates a protein called Mei3, which inhibits Pat1 to promote meiosis induction (30). The h^+/h^- cells 3 h after the induction were analysed, as fluorescence-activated cell sorting analyses showed that these cells were at a stage similar to that of *pat1-114* haploid cells 1 h after induction (data not shown). ChIP experiments confirmed that the higher H3K9ac and

lower H3K4me3 were associated with *M26* rather than *M375* (Figure 2E–G) ($P = 0.0051$ for K9ac; $P = 0.0088$ for K4me3). Therefore, *pat1-114* haploid meiosis and diploid meiosis gave similar results, supporting the relevance of the histone modification patterns obtained with the *pat1-114* system. Collectively, we conclude that high H3K9 acetylation, but not H3K4 trimethylation, is a characteristic of *M26*-sequence-dependent hotspots.

Interestingly, these patterns were already established at *ade6-M26* before entering meiosis (Supplementary Figure S6), similarly to what was previously observed at hotspot-associated H3K4me3 in budding yeast (12). Along with recent reports that nucleosome-free regions around hotspots are already seen in growing budding and fission yeast cells (5,6,13), hotspot-associated chromatin traits in these yeasts are not consequences caused by meiotic recombination, but rather, may be determined by factors present under pre-meiotic growth conditions.

Histone modification patterns observed around *M26*-sequence-dependent hotspots are distinct from those at an *M26*-sequence-dependent transcription promoter of *ctt1*$^+$

The *M26*-sequence and Atf1-Pcr1 also regulate the transcription of various genes, such as those involved in stress responses (31). Transcription is initiated also from *ade6-M26* and *ade6-3049*, but not from their corresponding sites in wild-type and negative control cells (32) (S. Y. K. O. and T. Y. unpublished observation), although its biological significance is unknown. These facts raise a possibility that the *ade6-M26* and *ade6-3049* hotspots can function as transcriptional promoters, and the histone modifications observed at *M26*-sequence-dependent hotspots may be shared with transcription, and not specific to recombination. To test this postulation, we focused on *M26*-dependent transcription that is not accompanied by recombination. The *ctt1*$^+$ is a good model for the following reasons. (i) It is induced by a high concentration of H_2O_2 in an Atf1-dependent manner (33). (ii) We found that mutations in the *M26*-sequence of its promoter (hereafter referred to as *ctt1-mut*) severely impaired Atf1 binding to the sequence and H_2O_2-induced transcription of *ctt1* (Figure 3A and Supplementary Figure S7A and B). (iii) The nearest Rec12 (the fission yeast homologue of Spo11)-DNA linkage site (29) and Rec12 binding site (Supplementary Figure S7C, see later in the text for the difference of Rec12-linkage sites and Rec12 binding sites) are both ~4 kb away from the *ctt1*$^+$ *M26*-sequence, indicating that this site is not close to meiotic recombination hotspots. We therefore activated transcription of *ctt1*$^+$ by treating vegetatively growing cells, in which meiotic recombination proteins such as Rec12 are not expressed, with 1 mM H_2O_2 for an hour. Histone modification levels were measured at its promoter (*Pctt1*$^+$) and at the mutated promoter (*Pctt1-mut*).

Under non-stressed conditions, we did not observe a substantial difference in histone H3 and its modification levels between *Pctt1*$^+$ and *Pctt1-mut*, although acetylation levels at K9 and K14 were slightly higher at *Pctt1-mut*

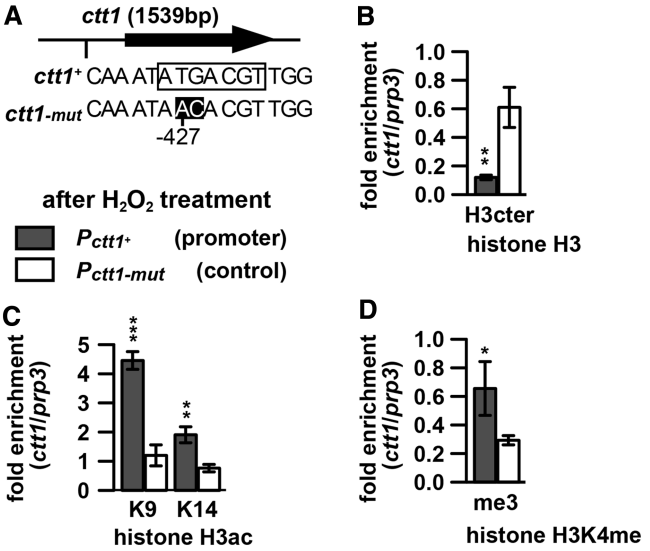

Figure 3. Histone modifications associated with transcriptional activation at the *ctt1*$^+$ promoter. Vegetatively growing *ctt1*$^+$ and *ctt1-mut* cells in a *pat1-114* background were treated with 1 mM H_2O_2 for an hour. (**A**) *M26*-sequence in the *ctt1*$^+$ promoter. Sequences around the upstream region of *ctt1* in *ctt1*$^+$ and *ctt1-mut* backgrounds are shown. The rectangle and white letterings indicate the *M26*-sequence and mutated bases, respectively. '−427' indicates the position of the mutated base (from 'T' to 'A'), with the first 'A' of the *ctt1* ORF as 1. Histone H3 and its modification levels were assessed by ChIP as in Figure 1H–J. (**B–D**) Total histone H3 and histone modification levels around *Pctt1*$^+$ (filled bars) and *Pctt1-mut* (open bars) after exposure to H_2O_2. (B) Levels of Histone H3. (C) Levels of H3K9ac and H3K14ac. (D) Levels of H3K4me3.

(Supplementary Figure S7D–F). After H_2O_2 treatment, however, histone levels plummeted at *Pctt1*$^+$ but stayed constant at *Pctt1-mut* (Figure 3B and Supplementary Figure S7D). Remarkably, in H_2O_2-treated cells, H3K9ac ($P = 0.00031$), H3K14ac ($P = 0.0029$) and H3K4me3 ($P = 0.028$) were all higher at *Pctt1*$^+$ than at *Pctt1-mut* (Figure 3C and D). These patterns are different from those observed at *M26*-sequence-dependent hotspots, as hotspots are not enriched with H3K4me3 compared with their respective controls. In summary, we infer that the modifications we observed at *M26*-sequence-dependent hotspots may not be caused solely by transcription from *M26*-sites but may be related to recombination.

Genome-wide analyses of histone modifications around meiotic recombination hotspots

Although the results described so far demonstrate a good correlation between histone modifications and recombination at *M26*-sequence-dependent hotspots, nearly 90% of fission yeast hotspots do not carry *M26*-sequence(s) around them (29). We therefore tested whether the modification patterns observed at *M26*-sequence-dependent hotspots are the general case by mapping histone H3, H3K9ac, H3K14ac, H3K4me3 and Rec12 across all three chromosomes of *S. pombe*.

To analyse the distribution of histone H3 and modified histones, *pat1-114* cells were harvested 1 h after meiosis

induction and were subjected to ChIP-chip experiments. In general, H3K9ac, H3K14ac and H3K4me3 localized at many sites where histone H3 level was reduced (Figure 4A–C). This finding is consistent with various prior observations that all these modifications are often found in open chromatin domains (2). In these domains, histone H3, present at lower level than the genome average and/or surrounding nucleosome-depleted regions, would be marked with the three modifications.

To map meiotic recombination hotspots, *pat1-114* haploid cells expressing Rec12 whose C-terminus is tagged with FLAG (Rec12-FLAG) were harvested 5 h after meiosis induction and processed for ChIP-chip analyses using anti-FLAG antibodies. This experiment was performed in the *rad50S* background, in which Rec12-induced DSBs accumulate so that we could avoid losing chromosome-bound Rec12 signals owing to prompt repair. We note that Rec12-FLAG is fully functional, as the tagged cells were proficient at DSB formation (Supplementary Figure S8A) and other meiotic events (34). The Rec12 binding map we obtained was in good accordance with a previously reported Rec12-DNA linkage map (29) (Supplementary Figure S12), despite the difference in experimental procedures (Hyppa *et al.* obtained a Rec12-DNA linkage map by ChIP, without cross-linkers, of the Rec12-FLAG protein covalently attached to DSB ends, whereas our Rec12 binding map was based on ChIP of Rec12-FLAG cross-linked to DNA by formaldehyde); thus, our Rec12 map can be considered to be a fission yeast hotspot map.

We first compared the distribution of histone H3 to that of Rec12 (Figure 4A). Consistent with a recent report (6), histone H3 anti-correlated with Rec12, which indicates that Rec12 binding sites are generally in regions with reduced nucleosomes (Figure 4E). This tendency is similar to that in budding yeast (5,13), but not in mouse (16). In the following experiments, data obtained with modified histones were normalized to histone H3cter values. Comparison between the Rec12 binding map and the H3K9ac and H3K14ac maps revealed that both modifications significantly overlapped with Rec12 peaks (Figure 4B). However, the extent of coincidence was much higher with H3K9ac than with H3K14ac; 81% (binomial test $P = 4.4 \times 10^{-47}$) and 46% ($P = 0.017$) of all Rec12 sites were enriched with H3K9ac and H3K14ac, respectively (Figure 4D, F and G). Moreover, only 15% of Rec12 peaks overlapped with H3K4me3 peaks, suggesting that H3K4me3 does not colocalize with DSB hotspots at a statistically meaningful level ($P = 1$) (Figure 4C, D and H). Most of H3K4me3-associated hotspots (48 of 49) were found around transcriptional promoters, and this may be similar to most of budding yeast hotspots (12,23). To provide more detailed information, close-up views around Rec12 hotspots are shown in Figure 4B (Supplementary Figure S8B), and several hotspots as well as *prp3*$^{+}$ control sites are also presented (Supplementary Figure S8C).

The immunoprecipitation ratio between modified histones and H3cter, usually a good indicator for histone modification levels, might not be relevant to evaluate modifications at hotspots, as hotspots are

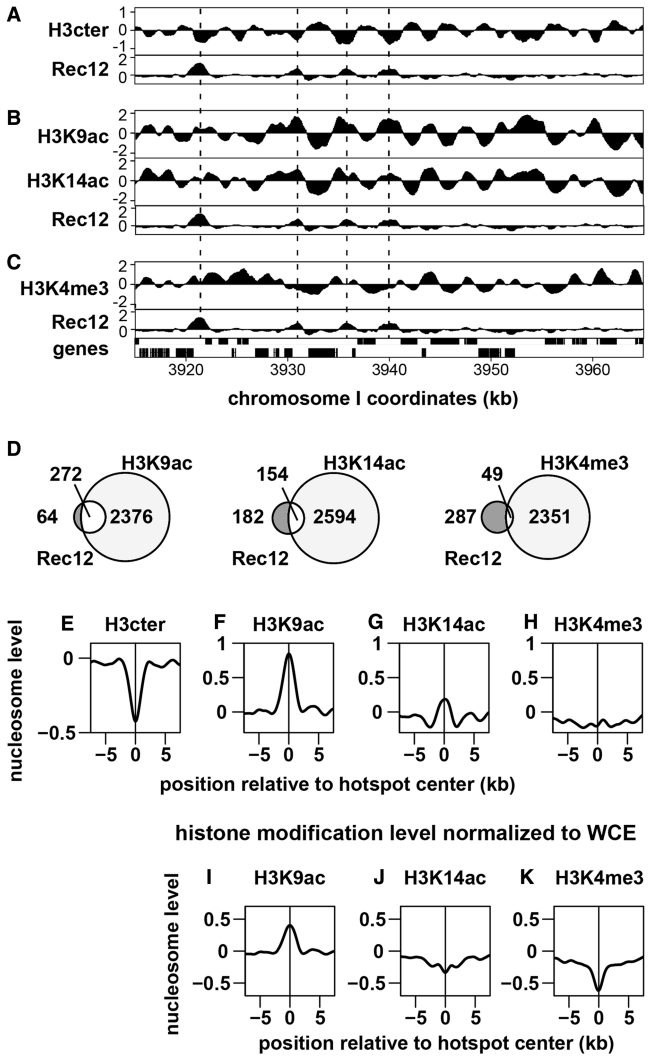

Figure 4. Genome-wide analysis of histone modifications around meiotic recombination hotspots. The *pat1-114* cells were induced into meiosis and harvested as in Figure 1. ChIP was performed using anti-histone H3, H3K9ac, H3K14ac and H3K4me3 antibodies, and the resultant DNA was analysed by GeneChip® *S. pombe* Tiling 1.0FR Array. The *pat1-114 rad50S rec12*$^{+}$*-FLAG* cells were induced into meiosis and harvested 5 h after the induction. ChIP was performed using anti-FLAG antibody, and the resultant DNA was similarly analysed. (**A–C**) Examples of ChIP-chip data. The *x*-axis shows the chromosomal coordinates in bp, and the *y*-axis shows the $\log_2$ of signal strength. The vertical dotted lines indicate Rec12 binding (i.e. DSB) sites. Genes are shown as filled boxes at the bottom of the figure. Comparison between Rec12 binding sites (Rec12) and histone H3 (H3cter; A), acetylated histone H3 (H3K9ac and H3K14ac; B) or trimetylated histone H3K4 (H3K4me3; C). Representative results are shown. Note that the levels of modified histones (B and C) are normalized to those of histone H3. (**D**) Venn diagrams showing the overlap between Rec12 binding (DSB) sites and modified histones calculated as described in 'Materials and Methods' section. (**E–K**) Distribution of histone H3 (E), H3K9ac (F and I), H3K14ac (G and J) and H3K4me3 (H and K) around meiotic recombination hotspots. The charts were created by a moving average method with a window size of 1 kb and a step size of 0.1 kb. The y axis shows the $\log_2$ of signal strength. The lines indicate the average of all hotspots. (F–H) Histone modification levels normalized to histone H3 were presented. (I–K) Histone modification levels normalized to whole-cell extract were presented.

generally associated with less nucleosomes. To consider this point, we normalized signals of modified histone immunoprecipitates to those of whole-cell extracts. These analyses revealed that H3K9ac (Figure 4I), but not H3K14ac (Figure 4J), is enriched in the centre of hotspots, and that the amount of H3K4me3 (Figure 4K) is reduced around hotspots.

These results provide important insights into fission yeast hotspot-associated modifications in general. (i) H3K9ac is associated with hotspots. (ii) H3K4me3 does not necessarily mark meiotic recombination hotspots. Therefore, histone modification patterns found in *M26*-sequence-dependent hotspots are not limited to *M26*-sequences; rather, they are generally associated with fission yeast hotspots.

Effects of mutation in H3K9 and deletion of *set1* on meiosis

Genome-wide histone modification analyses led us to assess the contribution of H3K9ac to meiotic recombination. We also analysed possible roles of H3K4me3, despite its absence at fission yeast hotspots, given its high occurrence at hotspots in mice and budding yeast. To this end, cells lacking either one of these modifications were created. A strain without H3K9ac was constructed by mutating all three histone H3 genes to change H3K9 to alanine (*H3K9A*) because multiple enzymes can acetylate H3K9. An H3K4me-deficient strain was obtained by deleting the $set1^+$ gene, which codes for the sole H3K4 methyltransferase (35). These strains were first tested for meiotic phenotypes.

Both *H3K9A* and *set1Δ* haploid cells in *pat1-114* h^- background arrested at G1 in response to nitrogen starvation, entered meiosis, and completed ensuing DNA replication without any abnormity (Supplementary Figure S9A), suggesting that neither H3K9ac nor H3K4me3 is required for G1 arrest followed by meiosis entry and pre-meiotic DNA synthesis. This result indicates that, in contrast to budding yeast, Set1 is dispensable for normal pre-meiotic DNA replication in fission yeast (14). Spore viability was also tested, and we found that it was reduced to about two-thirds of the wild-type level by *H3K9A* mutation ($P = 0.000012$), while it was largely unaffected by the *set1* deletion (Supplementary Figure S9B).

Meiotic recombination frequency was next analysed in the *H3K9A* and *set1Δ* mutants. We found that the *H3K9A* mutation, but not *set1* deletion, increases the frequency of conversion from h^+ cells to *M* cells (data not shown). This phenotype might be because the mutation disrupted heterochromatin structure at the mating-type locus. As such a defect hampers the analysis of recombination frequency, we crossed, instead of h^+ cells, *P* cells whose entire *mat2/3* interval is removed (*mat1*-P *mat2,3Δ::LEU2*) (36) to h^- cells. Gene conversion frequencies at *ade6-M26* were first tested by checking adenine prototrophy of spores derived from *ade6-M26* and *ade6-M210* parental strains. The analyses revealed that the *H3K9A* mutation reduced recombination frequency to less than half of wild-type cells (Supplementary Figure S9C). This result, along with the finding that H3K9ac is enriched at *ade6-M26* (Figure 1C and I), suggests that this modification would positively regulate recombination. Intriguingly, deletion of *set1* gene also decreased gene conversion at *M26* to a similar extent with *H3K9A*. As the H3K4me3 level is not elevated at *M26* than its control locus (Figure 1G and J), Set1 would facilitate recombination independently of H3K4me3. Next, the genetic distance between *ade6-arg1* (~299 kb region containing seven Rec12 binding sites, Supplementary Figure S12) was measured by crossing *ade6-M210* and *arg1-230* in wild-type, *H3K9A* and *set1Δ* backgrounds. We observed a partial, but significant, reduction in recombination activity in the *H3K9A* mutants ($P = 0.0018$) and the *set1Δ* mutants ($P = 0.020$) (Supplementary Figure S9D). The effects of *H3K9A* were stronger than those of *set1Δ*. These results show that both H3K9ac and Set1 are involved in meiotic recombination.

Effects of mutation in H3K9 and deletion of *set1* on Rec12 binding to chromatin

The aforementioned results, showing that *H3K9A* mutation and *set1* deletion reduced recombination at several sites, prompted us to analyse the effects of the mutations more thoroughly. To this end, we focused on early recombination events such as the loading of Rec12 to hotspots and meiotic DSB formation.

Distribution of Rec12 binding sites was tested by ChIP-chip analyses, as in Figure 4. Figure 5A compares the Rec12 binding maps of wild-type, *H3K9A* and *set1Δ* cells. Remarkably, the *H3K9A* mutation mildly reduced Rec12 signals at most of the hotspots without changing overall hotspot distribution patterns (Figure 5B). The average magnitude of this reduction was ~20% (Figure 5D). Although the impact of the *H3K9A* mutation was relatively modest, they were significant because two independent cultures of wild-type cells showed only a slight difference in hotspot-associated Rec12 levels (Supplementary Figure S10A–C). To our surprise, *set1* deletion generally increased Rec12 binding to hotspots (Figure 5C), and analyses of total hotspots revealed that Rec12 ChIP signals were 20% higher in the *set1Δ* mutant than in wild-type cells (Figure 5D).

To complement the genome-wide analyses, ChIP-qPCR at several loci (Figure 5E–I) were performed. At *hsp10* and *moc3* hotspots (Figure 5E and F), Rec12 levels were significantly reduced in the *H3K9A* mutant ($P = 0.0098$ at *hsp10*; $P = 0.027$ at *moc3*), confirming that H3K9ac positively regulate Rec12 localization at these hotspots. At *mbs1* locus (Figure 5G), we did not see an apparent change in Rec12 levels in the *H3K9A* mutants. However, we speculate that several acetylated-lysines including H3K9ac might redundantly function at this site, as lack of Gcn5, which acetylates multiple lysines on histones, decreased Rec12 levels (Supplementary Figure S10D). We also ascertained that *set1* deletion increases Rec12 binding at some sites, which are not categorized as hotspots in wild-type cells such as *vht1* (Figure 5H) and *mug160* (Figure 5I). It could be possible that Rec12 protein levels differ between wild-type and the mutant cells and affect interpretation of ChIP-chip results. However, we observed that comparable

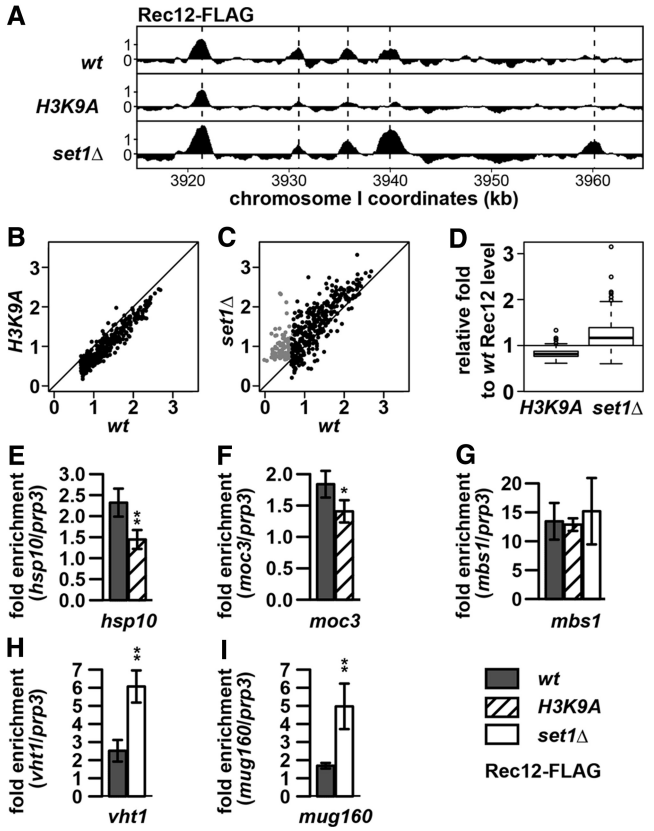

Figure 5. Effects of *H3K9A* mutation and *set1* deletion on Rec12 distribution. (**A–D**) The *pat1-114 rad50S rec12*$^{+}$*-FLAG* cells in the *H3K9A* or *set1Δ* backgrounds were induced into meiosis and analysed as in Figure 4. (A) Examples of ChIP-chip data. The *x*-axis shows the chromosomal coordinates in bp, and the *y*-axis shows the $\log_2$ of signal strength. The same chromosomal region with Figure 4A–C is shown. The vertical dotted lines indicate Rec12 binding sites. Representative results are shown. (B and C) Scatter plot comparing Rec12 levels in wild-type (*x*-axis) and the mutant (*y*-axis) based on the maximum signal strength ($\log_2$) of each Rec12 binding site. Rec12 binding sites that are present and absent in wild-type cells are shown in black and grey dots, respectively. (B) *H3K9A*. (C) *set1Δ*. The positions of *mbs1*, *mbs2* and *cds1* are presented in Supplementary Figure S10E. (D) Box-and-Whisker plots showing the ratio of Rec12 levels between the mutant and the wild-type, based on their respective maximum signal strengths of Rec12 binding sites present in wild-type cells. (**E–I**) ChIP-qPCR of Rec12-FLAG in wild-type, *H3K9A* or *set1Δ* cells. *pat1-114 rad50S rec12*$^{+}$*-FLAG* cells were induced into meiosis, harvested 5 h after the induction and analysed by ChIP-qPCR using anti-FLAG antibody. (E–G) Hotspots were analysed at *hsp10* (E), *moc3* (F) and *mbs1* (G). (H and I) Rec12 binding sites present only in *set1Δ* cells were analysed. *vht1* (H) and *mug160* (I).

amounts of Rec12 were expressed and immunoprecipitated from wild-type, *H3K9A* and *set1Δ* cells (Supplementary Figure S10F). Collectively, our analyses suggest that H3K9ac play some roles to facilitate Rec12 binding to hotspots and could have the potential to directly activate recombination. Set1 seems to restrict the access of Rec12 to a majority of hotspots, despite the fact that H3K4me3 is not enriched at hotspots.

Effects of mutation in H3K9 and deletion of *set1* on DSB formation

Finally, we set out to test the roles of H3K9ac and Set1 in meiotic DSB formation. Genomic DNA was extracted during meiotic progression and analysed by pulsed-field gel electrophoresis. For a rough estimation, DSBs formed on chromosomes were visualized by ethidium bromide staining (Figure 6A). In wild-type cells, smears reflecting Rec12-induced DSBs were observed ~3.5 h after meiosis induction. They intensified as meiosis proceeded, whereas signals of unbroken three chromosomes concomitantly disappeared. Intriguingly, the *H3K9A* mutation and *set1* deletion partially reduced DSB formation, as evidenced by the presence of intact chromosomes at 4.5 and 5 h (Figure 6A, 4.5 and 5 h in *H3K9*A and *set1Δ*). We also noticed that DSB signals at 3.5 h in the *H3K9A* mutant is reproducibly weaker than in wild-type cells (Figure 6A, 3.5 h; arrowheads), implying that DSB formation may be delayed by the *H3K9A* mutation. Consistent with the result in Figure 6A, Rec12-oligonucleotide complexes, another measure of the relative frequency of meiotic DSB (37), were less abundant in the *H3K9A* and the *set1Δ* mutants than in wild-type cells (Figure 6B, Supplementary Figure S11A and B), whereas Rec12 proteins were equally expressed and immunoprecipitated in wild-type and mutant cells. These results further indicate that H3K9ac and Set1 can facilitate DSB formation. It is also noteworthy that the complexes were consistently less detected in the *set1Δ* cells than the *H3K9A* cells at later stages, suggesting that Set1 might also function in other processes than DSB formation, such as releasing Rec12-oligonucleotides.

To quantitatively evaluate the DSB levels in the mutants, DSBs formed around several hotspots were analysed at a higher resolution using genomic DNA purified as in Figure 6A. The DSB signals at *mbs1* and *mbs2* were weaker in *H3K9A* mutants than in wild-type cells, and the defect was more obvious at the onset of DSB formation (Figure 6C and D). This result, together with our ChIP-chip data showing enrichment of H3K9ac at *mbs1* and *mbs2* (Supplementary Figure S8C), suggests that H3K9ac may be directly involved in DSB formation at hotspots. At the *cds1*$^{+}$ hotspot, DSB levels were reduced in the *H3K9A* mutant to <50% of wild-type cells (Figure 6E and F). Similarly, DSB formation was substantially impaired at the *hsp10* (Supplementary Figure S11C and D) and the *ade6-M26* (data not shown) hotspots. Like *mbs1* and *mbs2*, H3K9ac was associated with these hotspots (Figures 1C and I, 2C and Supplementary Figure S8C) and may at least partly facilitate DSB formation. In addition, these experiments also suggest that factors other than hotspot-associated H3K9ac are involved in DSB formation, as the effects of the *H3K9A* mutation were partial in many cases.

The *set1Δ* cells showed more intricate phenotypes. DSB levels in this mutant were comparable with wild-type cells at *mbs2* and at one site of *cds1*, but lower at *mbs1*, the other site of *cds1*, and *hsp10* (Figure 6C–F and Supplementary Figure S11C and D), indicating that the effects of *set1* deletion may vary among hotspot loci. Remarkably, as H3K4me3 was not elevated around *mbs1*, *hsp10* (Supplementary Figure S8C) and *cds1* (Figure 2D), Set1 would contribute to DSB formation at these loci independently of H3K4me3. Taken together, we infer

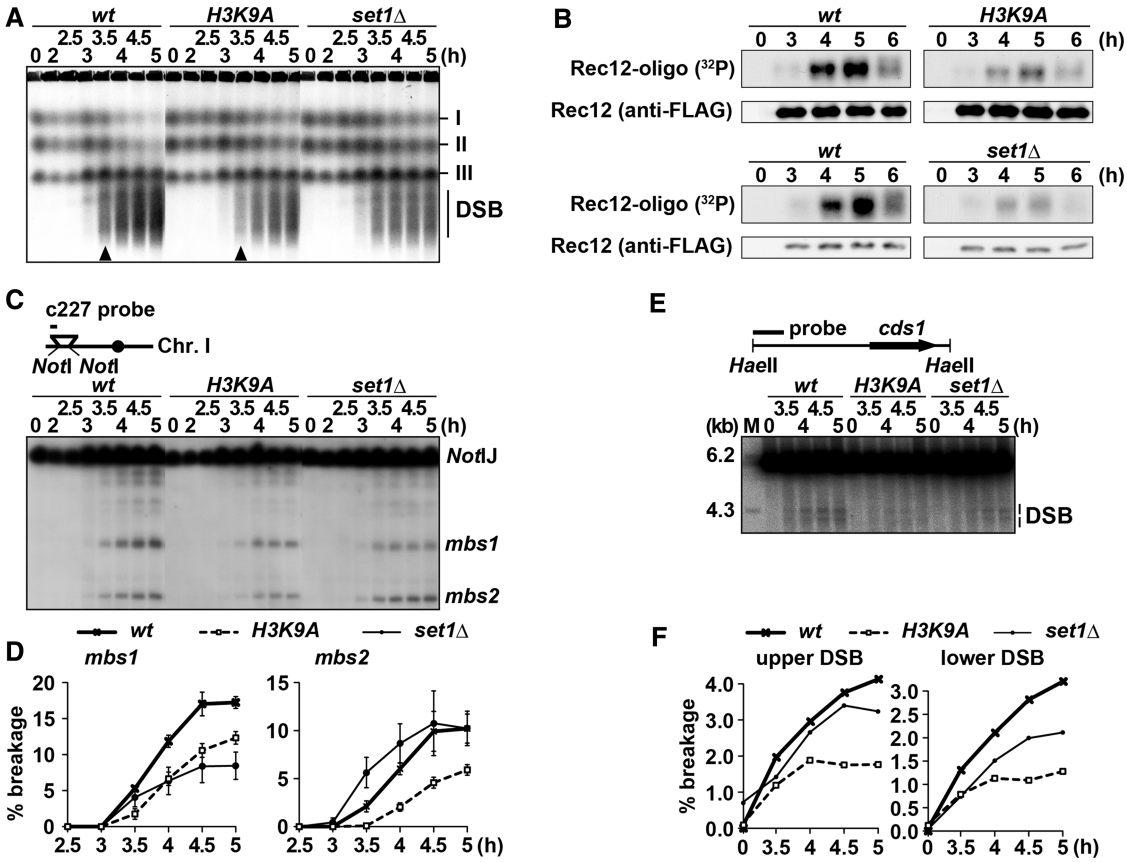

Figure 6. Effects of *H3K9A* mutation and *set1* deletion on meiotic DSB formation. (**A**, and **C–F**) The *pat1-114 rad50S* cells were induced into meiosis and were collected at indicated times after the induction. Genomic DNA was analysed by pulse-field gel electrophoresis (A) or standard gel electrophoresis (C–F). (**B**) The *pat1-114 rec12*$^{+}$*-FLAG* cells induced into meiosis and were collected at indicated times after the induction. Rec12-FLAG was immunoprecipitated and labelled with TdT and [α-^{32}P]dCTP. (A) Formation of meiotic DSBs at the chromosome level. DNA was visualized with ethidium bromide. The positions of chromosomes I, II, III and smears resulting from meiotic DSBs are shown. Note that the intact chromosomes are present at 4.5 and 5 h in the *H3K9A* and *set1Δ* mutants, but not in wild-type cells. The arrowheads indicate the point at which the delay in DSB formation of *H3K9A* was the most apparent (3.5 h). (B) Production of Rec12-oligonucleotide complexes is defective in the *H3K9A* and *set1Δ* mutants. ^{32}P-labelled Rec12-oligonucleotide complex and Rec12 were detected by autoradiography (^{32}P) and western blotting using horseradish peroxidase-conjugated anti-FLAG antibody (anti-FLAG), respectively. (C) An example showing the meiotic DSBs formed at *mbs1* and *mbs2*. DNA digested with *Not* I restriction endonuclease was analysed by Southern blotting with the c227 probe recognizing the left end of the *Not* I J fragment. (D) Quantification of the DSBs at *mbs1* and *mbs2*. These values were obtained by dividing the signal intensity of broken DNA fragments over the signal intensity of the unbroken *Not* I J fragment. The means and standard deviations from three independent experiments are shown. (E) An example showing the meiotic DSBs formed at *cds1*. DNA digested with *Hae* II restriction endonuclease was analysed by Southern blotting as described in (25). (F) Quantification of the DSBs at *cds1*. The experiment was performed twice to check reproducibility, and a representative result is shown.

that H3K9ac at hotspots may play some roles in DSB formation, and that Set1 may also enhance the process in some loci by a mechanism distinct from H3K9ac.

DISCUSSION

Recent studies showed that meiotic recombination hotspots are enriched with various histone modifications (12,16,20). However, hotspot-associated modifications are not fully identified yet, and their roles in recombination activation remain obscure. Here, using fission yeast, we studied hotspot-associated modifications and examined their possible roles in meiotic recombination.

Hotspot-associated histone modifications in fission yeast and other species

One of the most important findings in this study is that H3K9ac is a major hotspot-associated modification in fission yeast. Although this mark has not been extensively studied in other organisms, it is conceivable that H3K9ac may be universally associated with hotspots in a broad range of species. In this regard, hotspots in budding yeast are generally enriched with H3K9ac (13), and H3K9 is also highly acetylated at the mouse hotspot *Psmb9* (15).

In contrast, H3K4me3 was not elevated around fission yeast hotspots. This differs from budding yeast and mice, in which a vast majority of hotspots has H3K4me3. Although the reason for this difference is currently unknown, the relation between hotspots and H3K4me3 may vary among species. For instance, between budding yeast and mouse, there is a striking difference in the distribution of hotspot-associated H3K4me3: very often found around transcription start sites in the former, but virtually not in the latter (16). Moreover, several higher eukaryotes such as plants and dogs do not contain a

functional Prdm9 gene in their genomes (38). These observations point to the importance of testing the presence of H3K4me at hotspots in various organisms.

Other modifications are also likely to be involved in meiotic recombination. Indeed, H3K9 methylation and histone H2A lysine5 acetylation levels are related to meiotic DSB formation in *Caenorhabditis elegans* (39,40). Comprehensive investigation is important to thoroughly understand the association of modified histones with meiotic recombination hotspots.

Mechanism of histone modifications around hotspots in fission yeast and other species

M26-sequence-dependent hotspots were more tightly associated with H3K9ac than with all other acetylated lysines tested and were not enriched with any degrees of H3K4me compared with their control sites. Such two characteristics may be established by a mechanism involving *M26*-sequence and Atf1-Pcr1, as modification levels were largely not affected by their relative location within the ORF (Figure 1I, J, S and T compare *M26* and *3049*). Most likely, as we proposed previously, Atf1-Pcr1 binding to the hotspot would recruit histone acetyltransferases to acetylate H3K9 (20). There may be other proteins that contribute to histone modifications at recombination hotspots, similarly to Atf1-Pcr1. For instance, two sequence-specific DNA-binding factors, C CAAT-binding factor and Rst2, were recently found to regulate the activity of so-called 'CCAAT' hotspots and 'oligo-C' hotspots, respectively (41).

Other organisms may also exploit sequence-specific DNA-binding factors to modify histones around hotspots. Seventy-three percent of mice hotspots (16) and ~40% of human hotspots (17) possess a binding sequence for the zinc finger domain of the histone methylase Prdm9, a strong candidate for introducing hotspot-associated H3K4me3 (42). In *Saccharomyces cerevisiae*, earlier works pointed out that sequence-specific DNA-binding transcription factors are involved in meiotic recombination (43). Therefore, as discussed by Wahls' laboratory, it may be a general feature among species that specific sequences and their cognate-binding factors regulate recombination through chromatin structure (44,45).

In fission yeast, hotspots associated with sequences for protein binding are thought to constitute only a fraction of the total hotspots (25,41), and, for most of the remaining hotspots, no motif sequences have been found so far. Nevertheless, fission yeast hotspots are generally enriched with H3K9ac rather than with H3K14ac and H3K4me3 (Figure 4). These observations may imply a possibility that modification patterns can be established in a sequence-independent manner. In this case, as histone acetylases and deacetylases control not only targeted acetylation at specific sites but also global acetylation of the whole genome (46), this kind of 'global' system may contribute to modifications observed at recombination hotspots. Alternatively, as Borde *et al.* (12) proposed for H3K4me3 at budding yeast hotspots, the low-level transcription around hotspots may facilitate acetylation of H3K9. Such notion is consistent with the presence of non-coding RNA emanating from significant populations of meiotic recombination hotspots (47). This 'sequence-independent' mechanism may be important for other organisms as well, as the binding of transcription factors, in *S. cerevisiae*, *per se* is not sufficient to predict DSB hotspots and other factor(s) are in all likelihood involved (5).

Roles of histones and their modifications in meiotic recombination

This study revealed several chromatin-related factors that are associated with hotspots and/or facilitate meiotic recombination. In this section, three of them are discussed in terms of their possible roles in recombination.

Histone H3 levels were generally low around hotspots. This finding is consistent with previous studies (6,11,48) and supports a notion that chromatin structure is less condensed at hotspots to allow the access of recombination factors. However, our present study provides additional insights into this concept. For example, the hotspot-surrounding nucleosome-less region spreads over a ~3-kb region (Figure 4E). This may reflect the fact that meiotic DSBs are clustered in a wide region often spanning 1–2 kb (6,49). Another finding is that the reduction of nucleosome occupancy is relatively modest (~25% lower than the genome average) (Figure 4E), which is at a similar level to budding yeast hotspots (5,13). This observation may imply that recombination activation requires only mild decrease of nucleosome levels. However, because DSB is formed only in a small fraction of cells in a population, we must also consider the possibility that reduction of hotspot-surrounding nucleosomes might be underestimated owing to the majority of cells, which do not undergo DSB formation. Moreover, previous studies demonstrated that MNase sensitivities around hotspots increase as meiosis proceeds. Therefore, at hotspots where DNA is actually cut, nucleosome depletion might be more prominent than we observed in this study. Further exploration is necessary to understand nucleosome positioning at hotspots.

Mutating H3K9 to alanine reduced Rec12 ChIP signals at most hotspots and impaired DSB formation, albeit its effects were not very strong. We infer that H3K9ac may at least partly stabilize and/or facilitate the association of Rec12 with hotspots to induce DSBs. In addition, considering that the *H3K9A* mutation reduced DSB at *mbs1* in which it did not affect Rec12 levels (Figures 5G and 6C and D), H3K9ac may also target DSB-inducing proteins other than Rec12. As H3K9ac binds the bromodomain (50), there are several possible mechanisms for how this modification exerts such effects. For example, chromatin-modifying proteins, many of which possess the domain, may interact with H3K9ac and create open chromatin regions so that Rec12 can stably interact with hotspots. In this scenario, low level of H3K4me3 at hotspots (Figures 1G, J, Q, T, 2D, G and 4K) may be important for chromatin modifiers to discriminate between hotspots and transcriptional promoters, as the latter is usually associated with both acetylated histones

and H3K4me3. Revealing the H3K9ac interacting factors would be a key step to understand the roles of the modification in meiotic recombination.

Given the high association of H3K9ac with hotspots, the modest phenotype of the *H3K9A* mutant is puzzling. These observations, however, may indicate that several redundant factors and/or back-up pathways are involved in meiotic recombination. In this respect, nucleosome level is decreased around hotspots (Figure 4E) (6). Moreover, lack of Gcn5, an acetyltransferase targeting multiple lysines on histones, causes apparent reduction of Rec12 levels at *mbs1* (Supplementary Figure S10D). Therefore, additional factors including reduced nucleosome levels or other modifications might compensate for the loss of H3K9ac in fission yeast. Identifying factors that function in parallel with H3K9ac will be crucial to understand fission yeast meiotic recombination. Such situation may be similar to the cases in Prdm9$^{-/-}$ mice and *set1Δ* budding yeast where substantial amount of DSBs are formed (12,21). Indeed, a recent report that Prdm9 knockout mice exploit promoter-associated H3K4me3 for meiotic recombination suggests that mice have at least two overlapping systems for H3K4me3-mediated meiotic recombination (22). As meiotic recombination is a pivotal process, it is not surprising that cells are endowed with multiple pathways to accomplish the reaction. At the same time, it should be pointed out that we cannot formally exclude the possibility that such modifications play merely minor roles in the process.

The *set1* deletion caused several intriguing phenotypes. For example, the absence of Set1 generally increased Rec12-chromatin interaction (Figure 5C, D, H and I) but partially reduced DSB formation (Figure 6A and B). In addition, a locus in which *set1* deletion increased DSB formation has not been found so far (data not shown). These seemingly contradictory results suggest that increase in chromatin-bound Rec12 does not always cause increase in DSB formation. This idea may be related to previous findings that a fraction of Spo11 (Rec12) actually engages in DSB formation (26,37), and support a notion that Spo11 activity is limited to safely control DSB (51). Another important phenotype of *set1Δ* cells is that DSB formation was impaired at some, but not all, sites (Figure 6 and Supplementary Figure S11C and D), and the affected loci were not associated with H3K4me3 (Supplementary Figure S8C). Therefore, Set1 appears to facilitate meiotic recombination in an H3K4me3-independent- and site-specific-manner. Such a regulation is obviously different from roles proposed in budding yeast, where Set1 trimethylates H3K4 at hotspots to activate recombination (12). Then, how is fission yeast Set1 involved in the reaction? One possibility is that increased chromatin binding of Rec12 could inhibit DSB formation at authentic hotspots. Considering that Set1, along with other subunits of the Set1 COMPASS complex, is implicated in various DNA-related events (52), Set1 might regulate recombination by limiting access of Rec12 to chromatin through chromosome structure. An alternative possibility is that the absence of Set1 may perturb transcriptional patterns, and, thus, behaviours of Rec12 and DSB are indirectly affected. Although this model is not consistent with normal progression of early meiosis (Supplementary Figure S9A) and wild-type level of DSB formation at *mbs2* (Figure 6C and D) in *set1Δ* cells, transcriptome analysis of the mutant may be important. In addition to DSB formation, the *set1* deletion affected production of Rec12-oligos even more strongly than the *H3K9A* mutation (Figure 6B, Supplementary Figure S11A and B). This result implies that Set1 may also be involved in DSB processing (26,53). Dissecting the multiple functions of Set1 and H3K4me in *S. pombe* meiosis is expected to be informative to understand meiotic recombination in other species.

The major findings of this study are that (i) H3K9ac is associated with fission yeast hotspots and (ii) the *H3K9A* mutation and *set1* deletion mildly, but significantly, affected Rec12-chromatin binding and DSB formation. These observations imply that multiple chromatin-related factors are involved in the regulation of meiotic recombination in various ways. At the same time, this study also sheds light on the importance of factors other than H3K9ac or precise roles of Set1. Not only further functional analyses of H3K9ac and Set1 but also identifying other factors will be important to understand the *in vivo* mechanism of meiotic recombination.

SUPPLEMENTARY DATA

Supplementary Data are available at NAR Online: Supplementary Tables 1 and 2, Supplementary Figures 1–12, Supplementary Materials and Methods and Supplementary References [54–56].

ACKNOWLEDGEMENTS

The authors thank Drs G. Smith, W. Steiner, K. Hirota, T. Miyoshi, C. Wilkinson, and the National Bio-Resource Project of the MEXT Japan for strains; Drs G. Smith and R. Hyppa for the protocol for detecting Rec12-oligonucleotides. The authors are grateful to Dr G. Smith for helpful discussion and advice, and, Dr E. Luk, and Ms J. Galipon for critical reading of the manuscript. The authors also thank Ms E. Takaya and Dr K. Kugou for technical help, and members of our laboratory for helpful discussion.

FUNDING

Grant-in-aid for Young Scientists (B) from the Ministry of Education, Culture, Sports, Science, and Technology of Japan to T.Y.); Grant-in-Aid for Scientific Research on Innovative Areas from the Ministry of Education, Culture, Sports, Science, and Technology of Japan (to K.O.); the Research Fellowship for Young Scientists from the Japan Society for the Promotion of Science (to S.Y.). Funding for open access charge: Grant-in-aid for Young Scientists (B) and Grant-in-Aid for Scientific Research on Innovative Areas from the Ministry of Education, Culture, Sports, Science, and Technology of Japan.

Conflict of interest statement. None declared.

REFERENCES

1. Bell,O., Tiwari,V.K., Thoma,N.H. and Schubeler,D. (2011) Determinants and dynamics of genome accessibility. *Nat. Rev. Genet.*, **12**, 554–564.
2. Rando,O.J. (2007) Global patterns of histone modifications. *Curr. Opin. Genet. Dev.*, **17**, 94–99.
3. Keeney,S. (2007) *Spo11 and the Formation of DNA Ddouble-Sstrand Breaks in Meiosis*. Springer-Verlag, Heidelberg, Germany.
4. Lichten,M. (2008) *Meiotic Chromatin: The Substrate for Recombination Initiation*. Springer-Verlag, Berlin.
5. Pan,J., Sasaki,M., Kniewel,R., Murakami,H., Blitzblau,H.G., Tischfield,S.E., Zhu,X., Neale,M.J., Jasin,M., Socci,N.D. *et al.* (2011) A hierarchical combination of factors shapes the genome-wide topography of yeast meiotic recombination initiation. *Cell*, **144**, 719–731.
6. de Castro,E., Soriano,I., Marin,L., Serrano,R., Quintales,L. and Antequera,F. (2012) Nucleosomal organization of replication origins and meiotic recombination hotspots in fission yeast. *EMBO J.*, **31**, 124–137.
7. Ponticelli,A.S., Sena,E.P. and Smith,G.R. (1988) Genetic and physical analysis of the *M26* recombination hotspot of *Schizosaccharomyces pombe*. *Genetics*, **119**, 491–497.
8. Szankasi,P., Heyer,W.D., Schuchert,P. and Kohli,J. (1988) DNA sequence analysis of the *ade6* gene of *Schizosaccharomyces pombe*. Wild-type and mutant alleles including the recombination hot spot allele *ade6-M26*. *J. Mol. Biol.*, **204**, 917–925.
9. Schuchert,P., Langsford,M., Kaslin,E. and Kohli,J. (1991) A specific DNA sequence is required for high frequency of recombination in the *ade6* gene of fission yeast. *EMBO J.*, **10**, 2157–2163.
10. Kon,N., Krawchuk,M.D., Warren,B.G., Smith,G.R. and Wahls,W.P. (1997) Transcription factor Mts1/Mts2 (Atf1/Pcr1, Gad7/Pcr1) activates the *M26* meiotic recombination hotspot in *Schizosaccharomyces pombe*. *Proc. Natl Acad. Sci. USA*, **94**, 13765–13770.
11. Mizuno,K., Emura,Y., Baur,M., Kohli,J., Ohta,K. and Shibata,T. (1997) The meiotic recombination hot spot created by the single-base substitution *ade6-M26* results in remodeling of chromatin structure in fission yeast. *Genes Dev.*, **11**, 876–886.
12. Borde,V., Robine,N., Lin,W., Bonfils,S., Geli,V. and Nicolas,A. (2009) Histone H3 lysine 4 trimethylation marks meiotic recombination initiation sites. *EMBO J.*, **28**, 99–111.
13. Zhang,L., Ma,H. and Pugh,B.F. (2011) Stable and dynamic nucleosome states during a meiotic developmental process. *Genome Res.*, **21**, 875–884.
14. Sollier,J., Lin,W., Soustelle,C., Suhre,K., Nicolas,A., Geli,V. and de La Roche Saint-Andre,C. (2004) Set1 is required for meiotic S-phase onset, double-strand break formation and middle gene expression. *EMBO J.*, **23**, 1957–1967.
15. Buard,J., Barthes,P., Grey,C. and de Massy,B. (2009) Distinct histone modifications define initiation and repair of meiotic recombination in the mouse. *EMBO J.*, **28**, 2616–2624.
16. Smagulova,F., Gregoretti,I.V., Brick,K., Khil,P., Camerini-Otero,R.D. and Petukhova,G.V. (2011) Genome-wide analysis reveals novel molecular features of mouse recombination hotspots. *Nature*, **472**, 375–378.
17. Myers,S., Bowden,R., Tumian,A., Bontrop,R.E., Freeman,C., MacFie,T.S., McVean,G. and Donnelly,P. (2010) Drive against hotspot motifs in primates implicates the PRDM9 gene in meiotic recombination. *Science*, **327**, 876–879.
18. Baudat,F., Buard,J., Grey,C., Fledel-Alon,A., Ober,C., Przeworski,M., Coop,G. and de Massy,B. (2010) PRDM9 is a major determinant of meiotic recombination hotspots in humans and mice. *Science*, **327**, 836–840.
19. Parvanov,E.D., Petkov,P.M. and Paigen,K. (2010) Prdm9 controls activation of mammalian recombination hotspots. *Science*, **327**, 835.
20. Yamada,T., Mizuno,K., Hirota,K., Kon,N., Wahls,W.P., Hartsuiker,E., Murofushi,H., Shibata,T. and Ohta,K. (2004) Roles of histone acetylation and chromatin remodeling factor in a meiotic recombination hotspot. *EMBO J.*, **23**, 1792–1803.
21. Hayashi,K. and Matsui,Y. (2006) Meisetz, a novel histone tri-methyltransferase, regulates meiosis-specific epigenesis. *Cell Cycle*, **5**, 615–620.
22. Brick,K., Smagulova,F., Khil,P., Camerini-Otero,R.D. and Petukhova,G.V. (2012) Genetic recombination is directed away from functional genomic elements in mice. *Nature*, **485**, 642–645.
23. Tischfield,S.E. and Keeney,S. (2012) Scale matters: the spatial correlation of yeast meiotic DNA breaks with histone H3 trimethylation is driven largely by independent colocalization at promoters. *Cell Cycle*, **11**, 1496–1503.
24. Young,J.A., Schreckhise,R.W., Steiner,W.W. and Smith,G.R. (2002) Meiotic recombination remote from prominent DNA break sites in *S. pombe*. *Mol. Cell*, **9**, 253–263.
25. Steiner,W.W. and Smith,G.R. (2005) Natural meiotic recombination hot spots in the *Schizosaccharomyces pombe* genome successfully predicted from the simple sequence motif *M26*. *Mol. Cell Biol.*, **25**, 9054–9062.
26. Milman,N., Higuchi,E. and Smith,G.R. (2009) Meiotic DNA double-strand break repair requires two nucleases, MRN and Ctp1, to produce a single size class of Rec12 (Spo11)-oligonucleotide complexes. *Mol. Cell Biol.*, **29**, 5998–6005.
27. Katou,Y., Kanoh,Y., Bando,M., Noguchi,H., Tanaka,H., Ashikari,T., Sugimoto,K. and Shirahige,K. (2003) S-phase checkpoint proteins Tof1 and Mrc1 form a stable replication-pausing complex. *Nature*, **424**, 1078–1083.
28. Ji,H., Jiang,H., Ma,W., Johnson,D.S., Myers,R.M. and Wong,W.H. (2008) An integrated software system for analyzing ChIP-chip and ChIP-seq data. *Nat. Biotechnol.*, **26**, 1293–1300.
29. Hyppa,R.W., Cromie,G.A. and Smith,G.R. (2008) Indistinguishable landscapes of meiotic DNA breaks in *rad50*$^{+}$ and *rad50S* strains of fission yeast revealed by a novel *rad50*$^{+}$ recombination intermediate. *PLoS Genet.*, **4**, e1000267.
30. Yamamoto,M. (1996) Regulation of meiosis in fission yeast. *Cell Struct. Funct.*, **21**, 431–436.
31. Chen,D., Toone,W.M., Mata,J., Lyne,R., Burns,G., Kivinen,K., Brazma,A., Jones,N. and Bahler,J. (2003) Global transcriptional responses of fission yeast to environmental stress. *Mol. Biol. Cell.*, **14**, 214–229.
32. Hirota,K., Mizuno,K., Shibata,T. and Ohta,K. (2008) Distinct chromatin modulators regulate the formation of accessible and repressive chromatin at the fission yeast recombination hotspot *ade6-M26*. *Mol. Biol. Cell*, **19**, 1162–1173.
33. Chen,D., Wilkinson,C.R., Watt,S., Penkett,C.J., Toone,W.M., Jones,N. and Bahler,J. (2008) Multiple pathways differentially regulate global oxidative stress responses in fission yeast. *Mol. Biol. Cell*, **19**, 308–317.
34. Miyoshi,T., Ito,M., Kugou,K., Yamada,S., Furuichi,M., Oda,A., Yamada,T., Hirota,K., Masai,H. and Ohta,K. (2012) A central coupler for recombination initiation linking chromosome architecture to S phase checkpoint. *Mol. Cell*, **47**, 722–733.
35. Noma,K. and Grewal,S.I. (2002) Histone H3 lysine 4 methylation is mediated by Set1 and promotes maintenance of active chromatin states in fission yeast. *Proc. Natl Acad. Sci. USA*, **99(Suppl. 4)**, 16438–16445.
36. Klar,A.J. and Miglio,L.M. (1986) Initiation of meiotic recombination by double-strand DNA breaks in *S. pombe*. *Cell*, **46**, 725–731.
37. Neale,M.J. and Keeney,S. (2009) End-labeling and analysis of Spo11-oligonucleotide complexes in *Saccharomyces cerevisiae*. *Methods Mol. Biol.*, **557**, 183–195.
38. Oliver,P.L., Goodstadt,L., Bayes,J.J., Birtle,Z., Roach,K.C., Phadnis,N., Beatson,S.A., Lunter,G., Malik,H.S. and Ponting,C.P. (2009) Accelerated evolution of the Prdm9 speciation gene across diverse metazoan taxa. *PLoS Genet.*, **5**, e1000753.
39. Reddy,K.C. and Villeneuve,A.M. (2004) *C. elegans* HIM-17 links chromatin modification and competence for initiation of meiotic recombination. *Cell*, **118**, 439–452.
40. Wagner,C.R., Kuervers,L., Baillie,D.L. and Yanowitz,J.L. (2010) *xnd-1* regulates the global recombination landscape in *Caenorhabditis elegans*. *Nature*, **467**, 839–843.

41. Steiner,W.W., Davidow,P.A. and Bagshaw,A.T. (2011) Important characteristics of sequence-specific recombination hotspots in *Schizosaccharomyces pombe*. *Genetics*, **187**, 385–396.
42. Grey,C., Barthes,P., Chauveau-Le Friec,G., Langa,F., Baudat,F. and de Massy,B. (2011) Mouse PRDM9 DNA-binding specificity determines sites of histone H3 lysine 4 trimethylation for initiation of meiotic recombination. *PLoS Biol*., **9**, e1001176.
43. Petes,T.D. (2001) Meiotic recombination hot spots and cold spots. *Nat. Rev. Genet*., **2**, 360–369.
44. Wahls,W.P. and Davidson,M.K. (2010) Discrete DNA sites regulate global distribution of meiotic recombination. *Trends Genet*., **26**, 202–208.
45. Wahls,W.P. and Davidson,M.K. (2011) DNA sequence-mediated, evolutionarily rapid redistribution of meiotic recombination hotspots. *Genetics*, **189**, 685–694.
46. Katan-Khaykovich,Y. and Struhl,K. (2002) Dynamics of global histone acetylation and deacetylation in vivo: rapid restoration of normal histone acetylation status upon removal of activators and repressors. *Genes Dev*., **16**, 743–752.
47. Wahls,W.P., Siegel,E.R. and Davidson,M.K. (2008) Meiotic recombination hotspots of fission yeast are directed to loci that express non-coding RNA. *PLoS One*, **3**, e2887.
48. Hirota,K., Steiner,W.W., Shibata,T. and Ohta,K. (2007) Multiple modes of chromatin configuration at natural meiotic recombination hot spots in fission yeast. *Eukaryot. Cell*, **6**, 2072–2080.
49. Cromie,G.A., Rubio,C.A., Hyppa,R.W. and Smith,G.R. (2005) A natural meiotic DNA break site in *Schizosaccharomyces pombe* is a hotspot of gene conversion, highly associated with crossing over. *Genetics*, **169**, 595–605.
50. Dhalluin,C., Carlson,J.E., Zeng,L., He,C., Aggarwal,A.K. and Zhou,M.M. (1999) Structure and ligand of a histone acetyltransferase bromodomain. *Nature*, **399**, 491–496.
51. Lange,J., Pan,J., Cole,F., Thelen,M.P., Jasin,M. and Keeney,S. (2011) ATM controls meiotic double-strand-break formation. *Nature*, **479**, 237–240.
52. Dehe,P.M. and Geli,V. (2006) The multiple faces of Set1. *Biochem. Cell Biol*., **84**, 536–548.
53. Rothenberg,M., Kohli,J. and Ludin,K. (2009) Ctp1 and the MRN-complex are required for endonucleolytic Rec12 removal with release of a single class of oligonucleotides in fission yeast. *PLoS Genet*., **5**, e1000722.
54. Murakami,H. and Nurse,P. (1999) Meiotic DNA replication checkpoint control in fission yeast. *Genes Dev*., **13**, 2581–2593.
55. Cervantes,M.D., Farah,J.A. and Smith,G.R. (2000) Meiotic DNA breaks associated with recombination in *S. pombe*. *Mol. Cell*., **5**, 883–888.
56. Hirota,K., Hasemi,T., Yamada,T., Mizuno,K.I., Hoffman,C.S., Shibata,T. and Ohta,K. (2004) Fission yeast global repressors regulate the specificity of chromatin alteration in response to distinct environmental stresses. *Nucleic Acids Res*., **32**, 855–862.